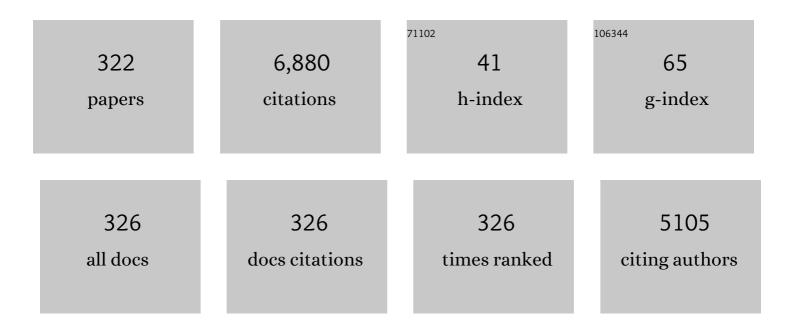
List of Publications by Year in descending order

Source: https://exaly.com/author-pdf/6482578/publications.pdf Version: 2024-02-01



POCED LECOMTE

#	Article	IF	CITATIONS
1	Initial results from the Sherbrooke avalanche photodiode positron tomograph. IEEE Transactions on Nuclear Science, 1996, 43, 1952-1957.	2.0	233
2	NEMA NU 4-2008 Comparison of Preclinical PET Imaging Systems. Journal of Nuclear Medicine, 2012, 53, 1300-1309.	5.0	191
3	<i>In vivo</i> measurement of energy substrate contribution to coldâ€induced brown adipose tissue thermogenesis. FASEB Journal, 2015, 29, 2046-2058.	0.5	183
4	Properties of LYSO and recent LSO scintillators for phoswich PET detectors. IEEE Transactions on Nuclear Science, 2004, 51, 789-795.	2.0	173
5	Respiratory gating for 3-dimensional PET of the thorax: feasibility and initial results. Journal of Nuclear Medicine, 2004, 45, 214-9.	5.0	143
6	Performance Evaluation of the LabPET APD-Based Digital PET Scanner. IEEE Transactions on Nuclear Science, 2009, 56, 10-16.	2.0	134
7	Investigation of depth-of-interaction by pulse shape discrimination in multicrystal detectors read out by avalanche photodiodes. IEEE Transactions on Nuclear Science, 1999, 46, 462-467.	2.0	123
8	Detector response models for statistical iterative image reconstruction in high resolution PET. IEEE Transactions on Nuclear Science, 2000, 47, 1168-1175.	2.0	111
9	RatCAP: miniaturized head-mounted PET for conscious rodent brain imaging. IEEE Transactions on Nuclear Science, 2004, 51, 2718-2722.	2.0	104
10	Novel detector technology for clinical PET. European Journal of Nuclear Medicine and Molecular Imaging, 2009, 36, 69-85.	6.4	104
11	Design and engineering aspects of a high resolution positron tomograph for small animal imaging. IEEE Transactions on Nuclear Science, 1994, 41, 1446-1452.	2.0	100
12	The Hardware and Signal Processing Architecture of LabPETâ,,¢, a Small Animal APD-Based Digital PET Scanner. IEEE Transactions on Nuclear Science, 2009, 56, 3-9.	2.0	100
13	A novel APD-based detector module for multi-modality PET/SPECT/CT scanners. IEEE Transactions on Nuclear Science, 1999, 46, 479-484.	2.0	98
14	Small-Animal PET: What Is It, and Why Do We Need It?. Journal of Nuclear Medicine Technology, 2012, 40, 157-165.	0.8	94
15	Metabolic activity of brown, "beige,―and white adipose tissues in response to chronic adrenergic stimulation in male mice. American Journal of Physiology - Endocrinology and Metabolism, 2016, 311, E260-E268.	3.5	92
16	Vascular-targeted photodynamic therapy with BF2-chelated Tetraaryl-Azadipyrromethene agents: a multi-modality molecular imaging approach to therapeutic assessment. British Journal of Cancer, 2009, 101, 1565-1573.	6.4	86
17	Image-derived input function in dynamic human PET/CT: methodology and validation with 11C-acetate and 18F-fluorothioheptadecanoic acid in muscle and 18F-fluorodeoxyglucose in brain. European Journal of Nuclear Medicine and Molecular Imaging, 2010, 37, 1539-1550.	6.4	86
18	Abnormal in vivo myocardial energy substrate uptake in diet-induced type 2 diabetic cardiomyopathy in rats. American Journal of Physiology - Endocrinology and Metabolism, 2010, 298, E1049-E1057.	3.5	82

#	Article	IF	CITATIONS
19	Endotoxin-induced heart dysfunction in rats: Assessment of myocardial perfusion and permeability and the role of fluid resuscitation*. Critical Care Medicine, 2006, 34, 127-133.	0.9	81
20	Geometry Study of a High Resolution PET Detection System Using Small Detectors. IEEE Transactions on Nuclear Science, 1984, 31, 556-561.	2.0	78
21	PET imaging of apoptosis with 64Cu-labeled streptavidin following pretargeting of phosphatidylserine with biotinylated annexin-V. European Journal of Nuclear Medicine and Molecular Imaging, 2007, 34, 247-258.	6.4	78
22	Design of a high resolution positron emission tomograph using solid state scintillation detectors. IEEE Transactions on Nuclear Science, 1988, 35, 685-690.	2.0	72
23	Measurement of the static quadrupole moments of the first 2+ states in 76Se, 78Se, 80Se and 82Se. Nuclear Physics A, 1977, 284, 123-134.	1.5	65
24	mTORC1 is Required for Brown Adipose Tissue Recruitment and Metabolic Adaptation to Cold. Scientific Reports, 2016, 6, 37223.	3.3	64
25	Investigation of CSO, LSO and YSO scintillators using reverse avalanche photodiodes. IEEE Transactions on Nuclear Science, 1998, 45, 478-482.	2.0	60
26	Technology challenges in small animal PET imaging. Nuclear Instruments and Methods in Physics Research, Section A: Accelerators, Spectrometers, Detectors and Associated Equipment, 2004, 527, 157-165.	1.6	57
27	Standardization and Detailed Characterization of the Syngeneic Fischer/F98 Glioma Model. Canadian Journal of Neurological Sciences, 2007, 34, 296-306.	0.5	56
28	Evidence of a spherical to prolate shape transition in the germanium nuclei. Physical Review C, 1980, 22, 1530-1533.	2.9	54
29	Coulomb-excitation studies ofGe70,Ge72,Ge74, andGe76. Physical Review C, 1980, 22, 2420-2423.	2.9	51
30	A New Tool for Molecular Imaging: The Microvolumetric Blood Counter. Journal of Nuclear Medicine, 2007, 48, 1197-1206.	5.0	51
31	PET study of ¹¹ C-acetoacetate kinetics in rat brain during dietary treatments affecting ketosis. American Journal of Physiology - Endocrinology and Metabolism, 2009, 296, E796-E801.	3.5	50
32	Quantitative gated PET for the assessment of left ventricular function in small animals. Journal of Nuclear Medicine, 2003, 44, 1655-61.	5.0	50
33	Quadrupole moments of the first excited states ofRu96,Ru98,Ru100,Ru102, andRu104. Physical Review C, 1980, 21, 588-594.	2.9	49
34	Behavioral, Medical Imaging and Histopathological Features of a New Rat Model of Bone Cancer Pain. PLoS ONE, 2010, 5, e13774.	2.5	49
35	Trace element analysis of freeze-dried blood serum by proton and alpha-induced X-rays. Nuclear Instruments & Methods, 1976, 134, 189-196.	1.2	48
36	Imaging performance of LabPET APD-based digital PET scanners for pre-clinical research. Physics in Medicine and Biology, 2014, 59, 661-678.	3.0	48

#	Article	IF	CITATIONS
37	System Architecture of the LabPET Small Animal PET Scanner. IEEE Transactions on Nuclear Science, 2008, 55, 2546-2550.	2.0	47
38	Status of BGO-avalanche photodiode detectors for spectroscopic and timing measurements. Nuclear Instruments and Methods in Physics Research, Section A: Accelerators, Spectrometers, Detectors and Associated Equipment, 1989, 278, 585-597.	1.6	46
39	EP 80317, a selective CD36 ligand, shows cardioprotective effects against post-ischaemic myocardial damage in mice. Cardiovascular Research, 2012, 96, 99-108.	3.8	46
40	Breast cancer models to study the expression of estrogen receptors with small animal PET imaging. Nuclear Medicine and Biology, 2004, 31, 761-770.	0.6	45
41	Architecture of a dual-modality, high-resolution, fully digital positron emission tomography/computed tomography (PET/CT) scanner for small animal imaging. IEEE Transactions on Nuclear Science, 2005, 52, 691-696.	2.0	45
42	Design and performance of 0.18-/spl mu/m CMOS charge preamplifiers for APD-based PET scanners. IEEE Transactions on Nuclear Science, 2004, 51, 1979-1985.	2.0	44
43	Fast point spread function computation from aperture functions in high-resolution positron emission tomography. IEEE Transactions on Medical Imaging, 1988, 7, 2-12.	8.9	43
44	The Effect of Insulin on the Intracellular Distribution of 14(R,S)-[18F]Fluoro-6-thia-heptadecanoic Acid in Rats. Molecular Imaging and Biology, 2006, 8, 237-244.	2.6	43
45	A Small Animal Positron Emission Tomography Study of the Effect of Chemotherapy and Hormonal Therapy on the Uptake of 2-Deoxy-2-[F-18]fluoro-d-glucose in Murine Models of Breast Cancer. Molecular Imaging and Biology, 2007, 9, 144-150.	2.6	43
46	Cross-validation stopping rule for ML-EM reconstruction of dynamic PET series: effect on image quality and quantitative accuracy. IEEE Transactions on Nuclear Science, 2001, 48, 883-889.	2.0	42
47	Quantitative myocardial perfusion and coronary reserve in rats with 13N-ammonia and small animal PET: impact of anesthesia and pharmacologic stress agents. Journal of Nuclear Medicine, 2004, 45, 1924-30.	5.0	42
48	High resolution positron emission tomography with a prototype camera based on solid state scintillation detectors. IEEE Transactions on Nuclear Science, 1990, 37, 805-811.	2.0	41
49	Radiation detection measurements with a new "Buried Junction―silicon avalanche photodiode. Nuclear Instruments and Methods in Physics Research, Section A: Accelerators, Spectrometers, Detectors and Associated Equipment, 1999, 423, 92-102.	1.6	41
50	The ketogenic diet increases brain glucose and ketone uptake in aged rats: A dual tracer PET and volumetric MRI study. Brain Research, 2012, 1488, 14-23.	2.2	41
51	Effect of geometrical modifications and crystal defects on light collection in ideal rectangular parallelepipedic BGO scintillators. Nuclear Instruments and Methods in Physics Research, Section A: Accelerators, Spectrometers, Detectors and Associated Equipment, 1990, 294, 355-364.	1.6	40
52	Front-end electronics for the RatCAP mobile animal PET scanner. IEEE Transactions on Nuclear Science, 2004, 51, 1318-1323.	2.0	40
53	⁶⁸ Ga/DOTA- and ⁶⁴ Cu/NOTA-Phthalocyanine Conjugates as Fluorescent/PET Bimodal Imaging Probes. Bioconjugate Chemistry, 2013, 24, 1624-1633.	3.6	40
54	Scintillation light emission studies of LSO scintillators. IEEE Transactions on Nuclear Science, 1999, 46, 1925-1928.	2.0	39

#	Article	IF	CITATIONS
55	Mild experimental ketosis increases brain uptake of ¹¹ C-acetoacetate and ¹⁸ F-fluorodeoxyglucose: a dual-tracer PET imaging study in rats. Nutritional Neuroscience, 2011, 14, 51-58.	3.1	37
56	Automatic data acquisition and on-line analysis of trace element concentration in serum samples. Nuclear Instruments & Methods, 1978, 150, 289-299.	1.2	36
57	Real time digital signal processing implementation for an APD-based PET scanner with phoswich detectors. IEEE Transactions on Nuclear Science, 2006, 53, 784-788.	2.0	36
58	Scintillation Detection with Large-Area Reach-Through Avalanche Photodiodes. IEEE Transactions on Nuclear Science, 1984, 31, 417-423.	2.0	35
59	Loss of UCP2 impairs cold-induced non-shivering thermogenesis by promoting a shift toward glucose utilization in brown adipose tissue. Biochimie, 2017, 134, 118-126.	2.6	34
60	Performance Characteristics of BGO-Silicon Avalanche Photodiode Detectors for PET. IEEE Transactions on Nuclear Science, 1985, 32, 482-486.	2.0	33
61	Conversion of arterial input functions for dual pharmacokinetic modeling using Gdâ€DTPA/MRI and ¹⁸ Fâ€FDG/PET. Magnetic Resonance in Medicine, 2013, 69, 781-792.	3.0	33
62	Measurement of the static quadrupole moments of the first2+states inMo94,Mo96,Mo98, andMo100. Physical Review C, 1976, 14, 835-841.	2.9	32
63	Theoretical modelling of light transport in rectangular parallelepipedic scintillators. Nuclear Instruments and Methods in Physics Research, Section A: Accelerators, Spectrometers, Detectors and Associated Equipment, 1990, 292, 685-692.	1.6	32
64	Recent results in scintillation detection with silicon avalanche photodiodes. IEEE Transactions on Nuclear Science, 1990, 37, 209-214.	2.0	32
65	Novel Radiolabeled Peptides for Breast and Prostate Tumor PET Imaging: ⁶⁴ Cu/and ⁶⁸ Ga/NOTA-PEG-[<scp>d</scp> -Tyr ⁶ ,βAla ¹¹ ,Thi ¹³ ,Nle <su Bioconjugate Chemistry, 2012, 23, 1687-1693.</su 	1 p> 1346 /su	p>] B BN(6–
66	LabPET II, an APD-based Detector Module with PET and Counting CT Imaging Capabilities. IEEE Transactions on Nuclear Science, 2015, 62, 756-765.	2.0	32
67	Improved Estrogen Receptor Assessment by PET Using the Novel Radiotracer ¹⁸ F-4FMFES in Estrogen Receptor–Positive Breast Cancer Patients: An Ongoing Phase II Clinical Trial. Journal of Nuclear Medicine, 2018, 59, 197-203.	5.0	32
68	Development of a 64-channel APD detector module with individual pixel readout for submillimetre spatial resolution in PET. Nuclear Instruments and Methods in Physics Research, Section A: Accelerators, Spectrometers, Detectors and Associated Equipment, 2009, 610, 20-23.	1.6	29
69	[11C]Acetate rest–stress protocol to assess myocardial perfusion and oxygen consumption reserve in a model of congestive heart failure in rats. Nuclear Medicine and Biology, 2012, 39, 287-294.	0.6	29
70	Design of a Real-Time FPGA-Based Data Acquisition Architecture for the LabPET II: An APD-Based Scanner Dedicated to Small Animal PET Imaging. IEEE Transactions on Nuclear Science, 2013, 60, 3633-3638.	2.0	29
71	Energy dependence of scatter components in multispectral PET imaging. IEEE Transactions on Medical Imaging, 1995, 14, 138-145.	8.9	28
72	Effect of detector weighting functions on the point spread function of high-resolution PET tomographs: a simulation study. IEEE Transactions on Medical Imaging, 1992, 11, 379-385.	8.9	27

#	Article	IF	CITATIONS
73	Real Time Implementation of a Wiener Filter Based Crystal Identification Algorithm. IEEE Transactions on Nuclear Science, 2008, 55, 925-929.	2.0	27
74	Crystal Identification Based on Recursive-Least-Squares and Least-Mean-Squares Auto-Regressive Models for Small Animal Pet. IEEE Transactions on Nuclear Science, 2008, 55, 2450-2454.	2.0	27
75	Comparative study of 64Cu/NOTA-[D-Tyr6,βAla11,Thi13,Nle14]BBN(6-14) monomer and dimers for prostate cancer PET imaging. EJNMMI Research, 2012, 2, 8.	2.5	27
76	Study of the resolution performance of an array of discrete detectors with independent readouts for positron emission tomography. IEEE Transactions on Medical Imaging, 1991, 10, 347-357.	8.9	26
77	Fast PET image reconstruction based on SVD decomposition of the system matrix. IEEE Transactions on Nuclear Science, 2001, 48, 761-767.	2.0	26
78	Performance analysis of phoswich/APD detectors and low-noise CMOS preamplifiers for high-resolution PET systems. IEEE Transactions on Nuclear Science, 2001, 48, 650-655.	2.0	26
79	Real Time Coincidence Detection Engine for High Count Rate Timestamp Based PET. IEEE Transactions on Nuclear Science, 2010, 57, 117-124.	2.0	26
80	Passivation of KMPR microfluidic channels with bovine serum albumin (BSA) for improved hemocompatibility characterized with metal-clad waveguides. Sensors and Actuators B: Chemical, 2012, 173, 447-454.	7.8	26
81	Metal chelate grafting at the surface of mesoporous silica nanoparticles (MSNs): physico-chemical and biomedical imaging assessment. Journal of Materials Chemistry B, 2015, 3, 748-758.	5.8	26
82	A Novel Positron Emission Tomography (PET) Approach to Monitor Cardiac Metabolic Pathway Remodeling in Response to Sunitinib Malate. PLoS ONE, 2017, 12, e0169964.	2.5	26
83	Object and detector scatter-function dependence on energy and position in high resolution PET. IEEE Transactions on Nuclear Science, 1995, 42, 1162-1167.	2.0	25
84	Real-Time Coincidence Detection System for Digital High Resolution APD-based Animal PET Scanner. , 0,		25
85	CT acquisition using PET detectors and electronics. IEEE Transactions on Nuclear Science, 2005, 52, 634-637.	2.0	25
86	Investigation of the LabPETâ,,¢ detector and electronics for photon-counting CT imaging. Nuclear Instruments and Methods in Physics Research, Section A: Accelerators, Spectrometers, Detectors and Associated Equipment, 2007, 571, 114-117.	1.6	25
87	Timing Improvement by Low-Pass Filtering and Linear Interpolation for the LabPET Scanner. IEEE Transactions on Nuclear Science, 2008, 55, 34-39.	2.0	25
88	Mono- and tri-cationic porphyrin-monoclonal antibody conjugates: photodynamic activity and mechanism of action. Immunology, 2011, 132, 256-265.	4.4	25
89	Sensitivity Increase Through a Neural Network Method for LOR Recovery of ICS Triple Coincidences in High-Resolution Pixelated- Detectors PET Scanners. IEEE Transactions on Nuclear Science, 2015, 62, 82-94.	2.0	25
90	Dynamic imaging of transient metabolic processes by small-animal PET for the evaluation of photosensitizers in photodynamic therapy of cancer. Journal of Nuclear Medicine, 2006, 47, 1119-26.	5.0	25

#	Article	IF	CITATIONS
91	Shape coexistence and shape transitions in the even-AGe nuclei. Physical Review C, 1982, 25, 2812-2814.	2.9	24
92	A microvolumetric blood counter/sampler for metabolic PET studies in small animals. IEEE Transactions on Nuclear Science, 1998, 45, 2195-2199.	2.0	24
93	The Architecture of LabTEP, a Small Animal APD-Based Digital PET Scanner. , 0, , .		24
94	Assessment of Cancer-Associated Biomarkers by Positron Emission Tomography: Advances and Challenges. Disease Markers, 2002, 18, 211-247.	1.3	23
95	Performance evaluation of the LabPET™ APD-based digital PET scanner. , 2007, , .		23
96	[11C] Acetoacetate Utilization by Breast and Prostate Tumors: a PET and Biodistribution Study in Mice. Molecular Imaging and Biology, 2008, 10, 217-223.	2.6	23
97	Time Determination of BGO-APD Detectors by Digital Signal Processing for Positron Emission Tomography. IEEE Transactions on Nuclear Science, 2009, 56, 2600-2606.	2.0	23
98	Modeling of Single Photon Avalanche Diode Array Detectors for PET Applications. IEEE Transactions on Nuclear Science, 2014, 61, 14-22.	2.0	23
99	The RatCAP Front-End ASIC. IEEE Transactions on Nuclear Science, 2008, 55, 2727-2735.	2.0	22
100	[11C]-Acetoacetate PET imaging: a potential early marker for cardiac heart failure. Nuclear Medicine and Biology, 2014, 41, 863-870.	0.6	22
101	Ultra-Low Noise Charge Sensitive Preamplifier for Scintillation Detection with Avalanche Photodiodes in PET Applications. IEEE Transactions on Nuclear Science, 1987, 34, 91-96.	2.0	21
102	Cardiac studies in rats with /sup 11/C-acetate and PET: a comparison with /sup 13/N-ammonia. IEEE Transactions on Nuclear Science, 2002, 49, 2322-2327.	2.0	21
103	Initial studies using the RatCAP conscious animal PET tomograph. Nuclear Instruments and Methods in Physics Research, Section A: Accelerators, Spectrometers, Detectors and Associated Equipment, 2007, 571, 14-17.	1.6	21
104	Radioisotopic Purity of Sodium Pertechnetate ^{99m} Tc Produced with a Medium-Energy Cyclotron: Implications for Internal Radiation Dose, Image Quality, and Release Specifications. Journal of Nuclear Medicine, 2015, 56, 1600-1608.	5.0	21
105	Reflectivity quenching of ESR multilayer polymer film reflector in optically bonded scintillator arrays. Nuclear Instruments and Methods in Physics Research, Section A: Accelerators, Spectrometers, Detectors and Associated Equipment, 2017, 851, 62-67.	1.6	21
106	A PET camera simulator with multispectral data acquisition capabilities. IEEE Transactions on Nuclear Science, 1993, 40, 1067-1074.	2.0	20
107	Mechanism of Reduced Myocardial Glucose Utilization During Acute Hypertriglyceridemia in Rats. Molecular Imaging and Biology, 2009, 11, 6-14.	2.6	20
108	PET imaging using 64Cu-labeled sulfophthalocyanines: Synthesis and biodistribution. Bioorganic and Medicinal Chemistry Letters, 2011, 21, 7470-7473.	2.2	20

#	Article	IF	CITATIONS
109	Angiotensin Il–Converting Enzyme Inhibition Improves Survival, Ventricular Remodeling, and Myocardial Energetics in Experimental Aortic Regurgitation. Circulation: Heart Failure, 2013, 6, 1021-1028.	3.9	20
110	Analytical model of DOI-induced time bias in ultra-fast scintillation detectors for TOF-PET. Physics in Medicine and Biology, 2019, 64, 065009.	3.0	20
111	Performance Simulation of an Ultrahigh Resolution Brain PET Scanner Using 1.2-mm Pixel Detectors. IEEE Transactions on Radiation and Plasma Medical Sciences, 2019, 3, 334-342.	3.7	20
112	[18F]-fluorodeoxyglucose positron emission tomography of the cat brain: A feasibility study to investigate osteoarthritis-associated pain. Veterinary Journal, 2015, 204, 299-303.	1.7	19
113	The loss of P2X7 receptor expression leads to increase intestinal glucose transit and hepatic steatosis. Scientific Reports, 2017, 7, 12917.	3.3	19
114	Characteristics of Lu\$_{1.8}\$Gd\$_{0.2}\$SiO\$_{5}\$:Ce (LGSO) for APD-Based PET Detector. IEEE Transactions on Nuclear Science, 2010, 57, 55-62.	2.0	18
115	Assessment of the Novel Estrogen Receptor PET Tracer 4-Fluoro-11β-methoxy-16α-[18F]fluoroestradiol (4FMFES) by PET Imaging in a Breast Cancer Murine Model. Molecular Imaging and Biology, 2013, 15, 625-632.	2.6	18
116	Real-Time Microfluidic Blood-Counting System for PET and SPECT Preclinical Pharmacokinetic Studies. Journal of Nuclear Medicine, 2016, 57, 1460-1466.	5.0	18
117	Static quadrupole moment of the first excited state ofSe74. Physical Review C, 1978, 18, 2801-2804.	2.9	17
118	Tuning of avalanche photodiode PET camera. IEEE Transactions on Nuclear Science, 1993, 40, 1062-1066.	2.0	17
119	Cardiac PET imaging of blood flow, metabolism, and function in normal and infarcted rats. IEEE Transactions on Nuclear Science, 2004, 51, 696-704.	2.0	17
120	Digital signal processing applied to crystal identification in Positron Emission Tomography dedicated to small animals. Nuclear Instruments and Methods in Physics Research, Section A: Accelerators, Spectrometers, Detectors and Associated Equipment, 2007, 571, 385-388.	1.6	17
121	[18F]-fluoroestradiol quantitative PET imaging to differentiate ER+ and ERα-knockdown breast tumors in mice. Nuclear Medicine and Biology, 2012, 39, 57-64.	0.6	17
122	Targeting IL-5Rα with antibody-conjugates reveals a strategy for imaging and therapy for invasive bladder cancer. Oncolmmunology, 2017, 6, e1331195.	4.6	17
123	Interscapular brown adipose tissue denervation does not promote the oxidative activity of inguinal white adipose tissue in male mice. American Journal of Physiology - Endocrinology and Metabolism, 2018, 315, E815-E824.	3.5	17
124	Trace Elements in Wet Atmospheric Deposition: Application and Comparison of PIXE, INAA, and Graphite-Furnace AAS Techniques. International Journal of Environmental Analytical Chemistry, 1983, 15, 89-106.	3.3	16
125	Timing performance of scintillators read out by silicon avalanche photodiodes. Nuclear Instruments and Methods in Physics Research, Section A: Accelerators, Spectrometers, Detectors and Associated Equipment, 1990, 299, 115-118.	1.6	16
126	Copper-64 labeled sulfophthalocyanines for positron emission tomography (PET) imaging in tumor-bearing rats. Journal of Porphyrins and Phthalocyanines, 2008, 12, 49-53.	0.8	16

#	Article	IF	CITATIONS
127	DOI estimation through signal arrival time distribution: a theoretical description including proof of concept measurements. Physics in Medicine and Biology, 2021, 66, 095015.	3.0	16
128	Total soluble and insoluble sulfur concentrations in urban snow. Environmental Science & Technology, 1983, 17, 542-546.	10.0	15
129	A Microvolumetric \$eta\$ Blood Counter for Pharmacokinetic PET Studies in Small Animals. IEEE Transactions on Nuclear Science, 2007, 54, 173-180.	2.0	15
130	A handy time alignment probe for timing calibration of PET scanners. Nuclear Instruments and Methods in Physics Research, Section A: Accelerators, Spectrometers, Detectors and Associated Equipment, 2009, 599, 113-117.	1.6	15
131	Assessment of \${m Lu}_{1.8}{m Gd}_{0.2}{m SiO}_{5}\$ (LCSO) Scintillators With APD Readout for PET/SPECT/CT Detectors. IEEE Transactions on Nuclear Science, 2010, 57, 1512-1517.	2.0	15
132	High spin states and band structure inRh99andRh101. Physical Review C, 1982, 26, 138-148.	2.9	14
133	Medium spin states inRu99andRu101. Physical Review C, 1983, 28, 1504-1518.	2.9	14
134	High Rate Photon Counting CT Using Parallel Digital PET Electronics. IEEE Transactions on Nuclear Science, 2008, 55, 40-47.	2.0	14
135	Development and Validation of a GATE Simulation Model for the LabPET Scanner. IEEE Transactions on Nuclear Science, 2009, 56, 3672-3679.	2.0	14
136	Determination of trace pollutants in urban snow using PIXE techniques. Nuclear Instruments & Methods in Physics Research, 1982, 193, 323-329.	0.9	13
137	Analytical study of the effect of collimation on the performance of PET cameras in 3-D imaging. IEEE Transactions on Nuclear Science, 1990, 37, 823-831.	2.0	13
138	Normalization of multispectral data in positron emission tomography. Physics in Medicine and Biology, 1993, 38, 1745-1760.	3.0	13
139	Initial Performance of the RatCAP, a PET Camera for Conscious Rat Brain Imaging. , 0, , .		13
140	Crystal Identification Based on Recursive-Least-Squares and Least-Mean-Squares AutoRegressive Models for Small-Animal PET. , 0, , .		13
141	System Integration of the LabPET Small Animal PET Scanner. , 2006, , .		13
142	Physical characterization of the LabPET& $\#x2122$; LGSO and LYSO scintillators. , 2007, , .		13
143	A Sub-Nanosecond Time Interval Detection System Using FPGA Embedded I/O Resources. IEEE Transactions on Nuclear Science, 2010, 57, 519-524.	2.0	13
144	Blood compatible microfluidic system for pharmacokinetic studies in small animals. Lab on A Chip, 2012, 12, 4683.	6.0	13

#	Article	IF	CITATIONS
145	Mammary Cancer Bone Metastasis Follow-up Using Multimodal Small-Animal MR and PET Imaging. Journal of Nuclear Medicine, 2013, 54, 944-952.	5.0	13
146	Fully 3D iterative CT reconstruction using polar coordinates. Medical Physics, 2013, 40, 111904.	3.0	13
147	Sensitivity in PET: Neural networks as an alternative to compton photons LOR analysis. , 2007, , .		12
148	Embedded real time digital signal processing unit for a 64-channel PET detector module. , 2011, , .		12
149	LabPET II, an APD-based PET detector module with counting CT imaging capability. , 2011, , .		12
150	Predicting efficacy of photodynamic therapy by real-time FDG-PET in a mouse tumour model. Photochemical and Photobiological Sciences, 2012, 11, 364-370.	2.9	12
151	Initial Evaluation of LabPET/SPECT Dual Modality Animal Imaging System. IEEE Transactions on Nuclear Science, 2013, 60, 76-81.	2.0	12
152	Clinical Trial with Sodium ^{99m} Tc-Pertechnetate Produced by a Medium-Energy Cyclotron: Biodistribution and Safety Assessment in Patients with Abnormal Thyroid Function. Journal of Nuclear Medicine, 2017, 58, 791-798.	5.0	12
153	Mouse Mast Cell Protease 4 Deletion Protects Heart Function and Survival After Permanent Myocardial Infarction. Frontiers in Pharmacology, 2018, 9, 868.	3.5	12
154	Trace element contamination in blood-collecting devices. International Journal of Nuclear Medicine and Biology, 1979, 6, 207-211.	0.3	11
155	Level structure ofKr79andKr81. Physical Review C, 1983, 27, 983-1002.	2.9	11
156	Fast, accurate and versatile Monte Carlo method for computing system matrix. , 2007, , .		11
157	Performance evaluation of the LabPET12, a large axial FOV APD-based digital PET scanner. , 2009, , .		11
158	Positron emission tomography detection of human endothelial cell and fibroblast monolayers: effect of pretreament and cell density on 18FDG uptake. Vascular Cell, 2012, 4, 5.	0.2	11
159	Endurance training or beta-blockade can partially block the energy metabolism remodeling taking place in experimental chronic left ventricle volume overload. BMC Cardiovascular Disorders, 2014, 14, 190.	1.7	11
160	On the use of the PIXE method to determine river water pollution in asbestos mining areas. The International Journal of Applied Radiation and Isotopes, 1979, 30, 261-262.	0.7	10
161	Asbestos pollution levels in river water measured by proton-induced X-ray emission (PIXE) techniques. Environmental Pollution Series B: Chemical and Physical, 1983, 5, 83-90.	0.7	10
162	Study of light collection in multi-crystal detectors. IEEE Transactions on Nuclear Science, 2000, 47, 1634-1639.	2.0	10

ROGER LECOMTE

#	Article	IF	CITATIONS
163	Wavelets-Based Crystal Identification of Phoswich Detectors for Small-Animal PET. IEEE Transactions on Nuclear Science, 2008, 55, 930-935.	2.0	10
164	Real Time Artificial Neural Network FPGA Implementation for Triple Coincidences Recovery in PET. IEEE Transactions on Nuclear Science, 2015, 62, 824-831.	2.0	10
165	NLS-Cholic Acid Conjugation to IL-5Rα-Specific Antibody Improves Cellular Accumulation and <i>In Vivo</i> Tumor-Targeting Properties in a Bladder Cancer Model. Bioconjugate Chemistry, 2018, 29, 1352-1363.	3.6	10
166	Trace element detection by the particle induced X-ray emission process. International Journal of Nuclear Medicine and Biology, 1981, 8, 1-16.	0.3	9
167	Design of a fast-shaping amplifier for PET/CT APD detectors with depth-of-interaction. IEEE Transactions on Nuclear Science, 2002, 49, 2448-2454.	2.0	9
168	Real Time Implementation of a Wiener Filter Based Crystal Identification Algorithm for Photon Counting CT Imaging. , 2006, , .		9
169	Accelerated iterative image reconstruction methods based on block-circulant system matrix derived from a cylindrical image representation. , 2007, , .		9
170	Time Discrimination Techniques Using Artificial Neural Networks for Positron Emission Tomography. IEEE Transactions on Nuclear Science, 2009, 56, 588-595.	2.0	9
171	Transcriptional Changes Associated with Long-Term Left Ventricle Volume Overload in Rats: Impact on Enzymes Related to Myocardial Energy Metabolism. BioMed Research International, 2015, 2015, 1-15.	1.9	9
172	Simulation of scintillation light output in LYSO scintillators through a full factorial design. Physics in Medicine and Biology, 2017, 62, 669-683.	3.0	9
173	Thermal cooling system development for LabPET II scanners by forced convection flow. , 2017, , .		9
174	Positron Emission Tomography Imaging of Tumor Response after Photodynamic Therapy. Journal of Environmental Pathology, Toxicology and Oncology, 2006, 25, 239-250.	1.2	9
175	Static quadrupole moment of the first2+state inMo98. Physical Review C, 1979, 20, 1201-1203.	2.9	8
176	Low-lying levels in 97Tc. Nuclear Physics A, 1980, 339, 238-252.	1.5	8
177	Performance evaluation of a dual-crystal APD-based detector modules for positron emission tomography. , 2006, 6142, 243.		8
178	The design and performance of the 2 nd -generation RatCAP awake rat brain PET system. , 2007, , .		8
179	A Fast Crystal Identification Algorithm Applied to the LabPETâ,,¢ Phoswich Detectors. IEEE Transactions on Nuclear Science, 2008, 55, 1644-1651.	2.0	8
180	Derivation of the system matrix for an animal SPECT scanner with rotational collimator and stationary ring detector. , 2010, , .		8

#	Article	IF	CITATIONS
181	Optimization and Calibration of Slat Position for a SPECT With Slit-Slat Collimator and Pixelated Detector Crystals. IEEE Transactions on Nuclear Science, 2011, 58, 2234-2243.	2.0	8
182	High efficiency microfluidic beta detector for pharmacokinetic studies in small animals. Nuclear Instruments and Methods in Physics Research, Section A: Accelerators, Spectrometers, Detectors and Associated Equipment, 2011, 652, 735-738.	1.6	8
183	Quantitative hormone therapy follow-up in an ER+/ERαKD mouse tumor model using FDG and [11C]-methionine PET imaging. EJNMMI Research, 2012, 2, 61.	2.5	8
184	Simplified size adjusted dose reference levels for adult CT examinations: A regional study. European Journal of Radiology, 2021, 142, 109861.	2.6	8
185	Experimental validation of a coincidence time resolution metric including depth-of-interaction bias for TOF-PET. Physics in Medicine and Biology, 2020, 65, 245004.	3.0	8
186	Asbestos pollution assessment in river water by PIXE methods. Nuclear Instruments & Methods, 1981, 181, 239-241.	1.2	7
187	Evaluation of trace-element sensitivities in PIXE analysis of low-temperature-ashed serum samples. The International Journal of Applied Radiation and Isotopes, 1982, 33, 121-125.	0.7	7
188	Dependence of the coincidence aperture function of narrow BGO crystals on crystal shape and light encoding schemes. Physics in Medicine and Biology, 1986, 31, 491-506.	3.0	7
189	A cross-correlation method for crystal identification in APD-based phoswich detectors used in small animal PET scanner. Nuclear Instruments and Methods in Physics Research, Section A: Accelerators, Spectrometers, Detectors and Associated Equipment, 2008, 597, 238-241.	1.6	7
190	Signal Deconvolution Concept Combined With Cubic Spline Interpolation to Improve Timing With Phoswich PET Detectors. IEEE Transactions on Nuclear Science, 2009, 56, 581-587.	2.0	7
191	Digital Identification of Fast Scintillators in Phoswich APD-Based Detectors. IEEE Transactions on Nuclear Science, 2010, 57, 1435-1440.	2.0	7
192	Firmware Upgrade for the Data Acquisition System of the LabPET Small Animal PET Scanner. IEEE Transactions on Nuclear Science, 2010, 57, 556-560.	2.0	7
193	Optimization of the reference region method for dual pharmacokinetic modeling using Gdâ€DTPA/MRI and ¹⁸ Fâ€FDG/PET. Magnetic Resonance in Medicine, 2015, 73, 740-748.	3.0	7
194	Postprandial fatty acid uptake and adipocyte remodeling in angiotensin type 2 receptor-deficient mice fed a high-fat/high-fructose diet. Adipocyte, 2016, 5, 43-52.	2.8	7
195	Performance evaluation of the mouse version of the LabPET II PET scanner. Physics in Medicine and Biology, 2021, 66, 065019.	3.0	7
196	Improvement of Spatial Resolution With Iterative PET Reconstruction Using Ultrafast TOF. IEEE Transactions on Radiation and Plasma Medical Sciences, 2021, 5, 729-737.	3.7	7
197	High spin states and band structure inTc97. Physical Review C, 1982, 26, 1462-1470.	2.9	6
198	Trapping of fluorescent light in cylindrical scintillators. Nuclear Instruments and Methods in Physics Research, Section A: Accelerators, Spectrometers, Detectors and Associated Equipment, 1989, 278, 622-624.	1.6	6

#	Article	IF	CITATIONS
199	Iterative CT reconstruction using LabPET™ detector modules. , 2008, , .		6
200	Monte Carlo results from neural networks as an alternative to Compton photons LOR analysis. , 2009, , .		6
201	ARMAX-RLS Parameter-Estimation Crystal Identification in Phoswich PET Detectors. IEEE Transactions on Nuclear Science, 2010, 57, 982-989.	2.0	6
202	Toward truly combined PET/CT imaging using PET detectors and photon counting CT with iterative reconstruction implementing physical detector response. Medical Physics, 2012, 39, 5697-5707.	3.0	6
203	Evaluation of easily implementable inter-crystal scatter recovery schemes in high-resolution PET imaging. , 2012, , .		6
204	Automatic Channel Fault Detection on a Small Animal APD-Based Digital PET Scanner. IEEE Transactions on Nuclear Science, 2014, 61, 2494-2502.	2.0	6
205	Impact of dianionic and dicationic linkers on tumor uptake and biodistribution of [⁶⁴ Cu]Cu/NOTA peptideâ€based gastrinâ€releasing peptide receptors antagonists. Journal of Labelled Compounds and Radiopharmaceuticals, 2017, 60, 200-212.	1.0	6
206	Studying the effects of metallic components of PET-insert on PET and MRI performance due to gradient switching. Physics in Medicine and Biology, 2019, 64, 075003.	3.0	6
207	A preclinical PET dual-tracer imaging protocol for ER and HER2 phenotyping in breast cancer xenografts. EJNMMI Research, 2020, 10, 69.	2.5	6
208	Monte Carlo simulations of energy, time and spatial evolution of primary electrons generated by 511ÂkeV photons in various scintillators. Nuclear Instruments and Methods in Physics Research, Section A: Accelerators, Spectrometers, Detectors and Associated Equipment, 2022, 1030, 166449.	1.6	6
209	Level structure ofTc97investigated via theMo97(p,Ânγ)reaction. Physical Review C, 1982, 26, 1451-1461.	2.9	5
210	Determination of sulphur in snow by proton induced X-ray emission (PIXE) method. Environmental Pollution Series B: Chemical and Physical, 1982, 3, 215-223.	0.7	5
211	Analytical study of performance in a 3D PET scanner. Physics in Medicine and Biology, 1992, 37, 623-634.	3.0	5
212	A stationary sampling scheme for multilayer positron tomographs. IEEE Transactions on Medical Imaging, 1993, 12, 293-298.	8.9	5
213	The RatCAP conscious small animal PET tomography. , 2005, , .		5
214	Roadmap to fully-digital PET/CT scanners. , 2007, , .		5
215	Biomedical Imaging: SPECT and PET. AIP Conference Proceedings, 2007, , .	0.4	5
216	LabPET II, a novel 64-channel APD-based PET detector module with individual pixel readout achieving submillimetric spatial resolution. , 2008, , .		5

#	Article	IF	CITATIONS
217	Imaging performance of the LabPET™ APD-based digital PET scanner. , 2008, , .		5
218	A fully integrated pulse charge generator embedded in a 64-channel readout ASIC dedicated to a PET/CT detector module. , 2012, , .		5
219	Improved LabPET Detectors Using <formula formulatype="inline"><tex notation="TeX">\${m Lu}_{1.8}{m Gd}_{0.2}{m SiO}_{5}!!:{m Ce}\$</tex></formula> (LGSO) Scintillator Blocks. IEEE Transactions on Nuclear Science, 2015, 62, 36-41.	2.0	5
220	Firmware architecture of the data acquisition system for the LabPET II mouse scanner. , 2016, , .		5
221	Scintillation and Spectroscopic Characteristics of 90%Lu LGSO With Variable Decay Times. IEEE Transactions on Radiation and Plasma Medical Sciences, 2017, 1, 23-29.	3.7	5
222	Cross-Species Physiological Assessment of Brain Estrogen Receptor Expression Using 18F-FES and 18F-4FMFES PET Imaging. Molecular Imaging and Biology, 2020, 22, 1403-1413.	2.6	5
223	TOF Benefits and Trade-offs on Image Contrast-to-Noise Ratio Performance for a Small Animal PET Scanner. IEEE Transactions on Radiation and Plasma Medical Sciences, 2021, 5, 687-693.	3.7	5
224	Dual-threshold Time-over-Threshold nonlinearity correction for PET detectors. Nuclear Instruments and Methods in Physics Research, Section A: Accelerators, Spectrometers, Detectors and Associated Equipment, 2020, 971, 164100.	1.6	5
225	Cross-validation of a non-invasive positron detector to measure the arterial input function for pharmacokinetic modelling in dynamic positron emission tomography. Physica Medica, 2020, 76, 92-99.	0.7	5
226	Elemental contamination in vacutainer tubes used for blood collection. International Journal of Nuclear Medicine and Biology, 1983, 10, 35-36.	0.3	4
227	Assessment of Quick-Stick 5870 high refractive index thermoplastic coupling compound. Nuclear Instruments and Methods in Physics Research, Section A: Accelerators, Spectrometers, Detectors and Associated Equipment, 2002, 488, 670-672.	1.6	4
228	Digital Coincidence Processing for the RatCAP Conscious Rat Brain PET Scanner. , 2006, , .		4
229	Cardiac PET image segmentation by a deformable model with a force field driven speed term. , 2008, , .		4
230	LabPET inter-crystal scatter study using GATE. , 2009, , .		4
231	New UV-enhanced, ultra-low noise silicon avalanche photodiode for radiation detection and medical imaging. , 2010, , .		4
232	Geometrical calibration for an animal PET converted SPECT. , 2010, , .		4
233	Design of a real-time FPGA-based DAQ architecture for the LabPET II, an APD-based scanner dedicated to small animal PET imaging. , 2012, , .		4
234	Arterial input function sampling without surgery in rats for positron emission tomography molecular imaging. Nuclear Medicine Communications, 2014, 35, 666-676.	1.1	4

#	Article	IF	CITATIONS
235	Scintillation characteristics of 90%Lu LGSO with different decay times. , 2014, , .		4
236	Performance characterization of a dual-threshold time-over-threshold APD-based detector front-end module for PET imaging. , 2015, , .		4
237	Optimization of Single Photon Avalanche Diode array detectors with a custom simulator. , 2015, , .		4
238	Initial Evaluation of Antibody-conjugates Modified with Viral-derived Peptides for Increasing Cellular Accumulation and Improving Tumor Targeting. Journal of Visualized Experiments, 2018, , .	0.3	4
239	A fully automated and scalable timing probe-based method for time alignment of the LabPET II scanners. Nuclear Instruments and Methods in Physics Research, Section A: Accelerators, Spectrometers, Detectors and Associated Equipment, 2018, 889, 1-6.	1.6	4
240	Estrogenic impregnation alters pain expression: analysis through functional neuropeptidomics in a surgical rat model of osteoarthritis. Naunyn-Schmiedeberg's Archives of Pharmacology, 2022, 395, 703-715.	3.0	4
241	On the use of PIXE as methodology for measuring asbestos pollution in river-water. The International Journal of Applied Radiation and Isotopes, 1981, 32, 122-125.	0.7	3
242	MLEM Reconstructed Image Resolution from the LabPET Animal Scanner. , 2006, , .		3
243	Novel CT detector based on an inorganic scintillator working in photon-counting mode. , 2006, , .		3
244	List-mode image reconstruction for real-time PET imaging. Journal of Visual Communication and Image Representation, 2006, 17, 630-646.	2.8	3
245	Performance Enhancement of the RatCAP Awake Rat Brain PET System. , 2006, , .		3
246	The RatCAP front-end ASIC. , 2007, , .		3
247	Timing improvement by low-pass filtering and linear interpolation for the LabPET TM scanner. , 2007, , .		3
248	Characteristics of Lu <inf>1.8</inf> Gd <inf>0.2</inf> SiO <inf>5</inf> :Ce (LGSO) for APD-based PET detector. , 2008, , .		3
249	Rapid prototyping of integrated microfluidic devices for combined radiation detection and plasma separation. , 2008, , .		3
250	Modeling of single photon avalanche diode array detectors for PET applications. , 2011, , .		3
251	Slit-slat collimator geometrical calibration for a PET/SPECT dual modality animal scanner. , 2011, , .		3
252	Deciphering PDT-induced inflammatory responses using real-time FDG-PET in a mouse tumour model. Photochemical and Photobiological Sciences, 2014, 13, 1434-1443.	2.9	3

#	Article	IF	CITATIONS
253	Automatic Channel Fault Detection and Diagnosis System for a Small Animal APD-Based <newline></newline> Digital PET Scanner. IEEE Transactions on Nuclear Science, 2015, 62, 1070-1076.	2.0	3
254	A real-time follow-up of photodynamic therapy during PET imaging. Photodiagnosis and Photodynamic Therapy, 2015, 12, 428-435.	2.6	3
255	Dichotomic effects of clinically used drugs on tumor growth, bone remodeling and pain management. Scientific Reports, 2019, 9, 20155.	3.3	3
256	Performance investigation of LabPET II detector technology in an MRI-like environment. Physics in Medicine and Biology, 2020, 65, 035001.	3.0	3
257	Effects of energy space smoothing and projection space normalization on multispectral PET image quality. IEEE Transactions on Nuclear Science, 1996, 43, 1988-1994.	2.0	2
258	A pulse simulator for crystal identification validation of phoswich detectors used in positron emission tomography. , 2009, 2009, 6942-5.		2
259	Reconstructed Image Resolution of the LabPET Small Animal Scanner Measured Using Simulated Partial Volume Effects. IEEE Transactions on Nuclear Science, 2009, 56, 2689-2695.	2.0	2
260	Results from neural networks for recovery of PET triple coincidences. , 2010, , .		2
261	Microfluidic beta and conversion electron radiation detector for preclinical pharmacokinetic studies with PET and SPECT radiotracers. , 2010, , .		2
262	Cylindrical and spherical ray-tracing for CT iterative reconstruction. , 2011, , .		2
263	Imaging performance of a PET/SPECT dual modality animal system. , 2011, , .		2
264	N-3 fatty acids, neuronal activity and energy metabolism in the brain. Oleagineux Corps Gras Lipides, 2012, 19, 238-244.	0.2	2
265	PET-based geometrical calibration of a pinhole SPECT add-on for an animal PET scanner. Physics in Medicine and Biology, 2013, 58, 2011-2025.	3.0	2
266	Comment on "Temperature dependence of APD-based PET scanners―[Med. Phys. 40(9) 092506 (13pp.) (2013)]. Medical Physics, 2013, 41, 017101.	3.0	2
267	A Longitudinal Low Dose <i>î¼</i> CT Analysis of Bone Healing in Mice: A Pilot Study. Advances in Orthopedics, 2014, 2014, 1-9.	1.0	2
268	Simulation of signal losses in highly pixelated scintillator arrays read out by discrete photodetectors. , 2015, , .		2
269	Revisiting motion compensation models in PET image reconstruction. , 2016, , .		2
270	Intratumoral 18F-FLT infusion in metabolic targeted radiotherapy. EJNMMI Research, 2019, 9, 33.	2.5	2

ROGER LECOMTE

#	Article	IF	CITATIONS
271	Investigation of a Model-Based Time-Over-Threshold Technique for Phoswich Crystal Discrimination. IEEE Transactions on Radiation and Plasma Medical Sciences, 2022, 6, 393-403.	3.7	2
272	Poster - 01: LabPET II Pixelated APD-Based PET Scanner for High-Resolution Preclinical Imaging. Medical Physics, 2016, 43, 4935-4935.	3.0	2
273	MRIâ€compatibility study of a PETâ€insert based on a lowâ€profile detection frontâ€end with submillimeter spatial resolution. Medical Physics, 2020, 47, 4396-4406.	3.0	2
274	Trace element analysis in rheumatoid arthritis under chrysotheraphy. Nuclear Instruments & Methods, 1981, 181, 301-303.	1.2	1
275	Pre-processing variance reducing techniques in multispectral positron emission tomography. Physics in Medicine and Biology, 1997, 42, 2233-2253.	3.0	1
276	Study of multispectral frame-by-frame convolution scatter correction in high resolution PET. IEEE Transactions on Nuclear Science, 1997, 44, 2489-2493.	2.0	1
277	A Microvolumetric β Blood Counter for Pharmacokinetic Pet Studies in Small Animals. , 0, , .		1
278	Kinetic modeling of PET data and FDG continuous infusion in rat tumors simultaneously treated with PDT. , 2007, , .		1
279	Comparison of analytical and algebraic 2D tomographic reconstruction approaches for irregularly sampled microCT data. Annual International Conference of the IEEE Engineering in Medicine and Biology Society, 2007, 2007, 2916-9.	0.5	1
280	Fast 3D image reconstruction method based on SVD decomposition of a block-circulant system matrix. , 2007, , .		1
281	ULTRA-Fast wiener filter based crystal identification algorithm applied to the LabPET TM phoswich detectors. , 2007, , .		1
282	High Rate Photon Counting CT Using Parallel Digital PET Electronics. , 2007, , .		1
283	Signal deconvolution concept combined with Cubic Spline interpolation to improve timing with phoswich pet detectors. , 2008, , .		1
284	Fast high lutetium content scintillators as candidates for APD-based phoswich detectors with depth-of-interaction (DOI). , 2009, , .		1
285	A Sub-Nanosecond Edge Detection System using embedded FPGA fabrics. , 2009, , .		1
286	Correction of partial volume effect in the projections in PET studies. , 2010, , .		1
287	Calibration process for improving Crystal Identification rate in the LabPET™ phoswich detectors. , 2010, , .		1
288	Slit-slat collimator geometrical calibration for a PET/SPECT dual modality animal scanner. , 2012, , .		1

288 Slit-slat collimator geometrical calibration for a PET/SPECT dual modality animal scanner. , 2012, , .

ROGER LECOMTE

#	Article	IF	CITATIONS
289	The Effect of Photon Statistics and Pulse Shaping on the Performance of the Wiener Filter Crystal Identification Algorithm Applied to LabPET Phoswich Detectors. IEEE Transactions on Nuclear Science, 2012, 59, 513-519.	2.0	1
290	Ultra-high sensitivity detection of bimodal probes at ultra-low noise for combined fluorescence and positron emission tomography imaging. , 2013, , .		1
291	A Dual Tracer PET-MRI Protocol for the Quantitative Measure of Regional Brain Energy Substrates Uptake in the Rat. Journal of Visualized Experiments, 2013, , 50761.	0.3	1
292	Automatic channel fault detection and diagnosis system for a small animal APD-based digital PET scanner. , 2014, , .		1
293	System architecture of a fully combined PET/CT scanner using LabPETâ,,¢ electronics with an upgraded analog front-end optimized for PET and CT counting mode operation. , 2015, , .		1
294	Initial results for automatic calibration of the LabPET II front-end detector module. , 2015, , .		1
295	Impacts of Intelligent Automated Quality Control on a Small Animal APD-Based Digital PET Scanner. IEEE Transactions on Nuclear Science, 2016, 63, 2550-2557.	2.0	1
296	A thermal model of the LabPET II ASIC. Nuclear Instruments and Methods in Physics Research, Section A: Accelerators, Spectrometers, Detectors and Associated Equipment, 2020, 953, 163142.	1.6	1
297	Thermal management proposal for a low-profile positron emission tomography fully pixelated front-end for submillimetric resolution MRI compatible insert dedicated to small animals. Nuclear Instruments and Methods in Physics Research, Section A: Accelerators, Spectrometers, Detectors and Associated Equipment, 2020, 966, 163848.	1.6	1
298	Annihilation Photon Acolinearity with Ultra-fast ToF-PET. , 2020, , .		1
299	Estimation of the Internal Dose Imparted by 18F-Fluorodeoxyglucose to Tissues by Using Fricke Dosimetry in a Phantom and Positron Emission Tomography. Frontiers in Nuclear Medicine, 2022, 2, .	1.2	1
300	Novel carbon nanotube-composite for electromagnetic shielding of radiation detectors: A step toward fully integrated positron emission tomography and magnetic resonance imaging systems. Microelectronic Engineering, 2022, 262, 111838.	2.4	1
301	Kinetic Modeling of FDG uptake in rat tumors During photodynamic therapy. , 2006, , .		0
302	Development and validation of a GATE simulation model for the LabPET scanner. , 2008, , .		0
303	PET kinetic modeling of rat tumors simultaneously treated with photodynamic therapy: A reference tissue model. , 2008, , .		0
304	LabPET pulse simulator for crystal identification validation of multi-layer phoswich detectors. , 2009, , .		0
305	Investigation of Lu <inf>1.8</inf> Gd <inf>0.2</inf> SiO <inf>5</inf> :Ce (LGSO) scintillators with APD readout for medical imaging applications. , 2009, , .		0
306	Firmware upgrade for the data acquisition system of the LabPET™ small animal PET scanner. , 2009, , .		0

#	Article	IF	CITATIONS
307	Improved LabPET detectors using Lu <inf>1.8</inf> Gd <inf>0.2</inf> SiO <inf>5</inf> :Ce (LGSO) scintillator blocks. , 2010, , .		О
308	An investigation of Lu <inf>1.8</inf> Gd <inf>0.2</inf> SiO <inf>5</inf> :Ce (LGSO) phoswich crystal identification by digital methods. , 2011, , .		0
309	Polyenergetic CT sinogram generator. , 2012, , .		0
310	Parameter optimization and effective imaging volume determination of helical scan for a pinhole animal SPECT. , 2012, , .		0
311	In situ positron emission tomography monitoring of endothelial cells embedded in perfused fibrin gels. Process Biochemistry, 2013, 48, 1645-1650.	3.7	Ο
312	Energy window optimization of PET detectors for SPECT imaging. , 2013, , .		0
313	Preliminary results of an automatic channel fault detection system on a small animal APD-based digital PET scanner. , 2013, , .		Ο
314	Keynote speakers: The challenges of pattern recognition for speech signals. , 2014, , .		0
315	Effect of inter-crystal scatter events on coincidence detection in LabPET scanners. , 2014, , .		Ο
316	Multipinhole SPECT helical scan parameters and imaging volume. Medical Physics, 2015, 42, 6599-6609.	3.0	0
317	Initial results of applying automatic channel fault detection and diagnosis on small animal APD-based digital PET scanners. , 2015, , .		0
318	Comparison of two motion compensation models: Adding ordered subset into the mix. , 2016, , .		0
319	Preliminary results of an embedded timing probe for calibrating PET scanner. , 2016, , .		Ο
320	Using Docker, an Industry Standard Technology to Run GATE Simulation on Multiple Platforms. , 2018, , .		0
321	Predicting Small Lesion Detectability for a Small Animal TOF PET Scanner. IEEE Transactions on Radiation and Plasma Medical Sciences, 2022, 6, 601-608.	3.7	0
322	The ultra high sensitivity blood counter: a compact, MRI-compatible, radioactivity counter for pharmacokinetic studies in µL volumes. Biomedical Physics and Engineering Express, 2022, , .	1.2	0